

Charge order induced by electron-lattice interaction in NaV_2O_5

B. Edegger,^{1,2} H. G. Evertz,¹ and R. M. Noack³

¹*Institut für Theoretische Physik, Technische Universität Graz, A-8010 Graz, Austria*

²*Institut für Theoretische Physik, Universität Frankfurt, D-60438 Frankfurt, Germany*

³*Fachbereich Physik, Philipps Universität Marburg, D-35032 Marburg, Germany*

(Received 31 May 2005; published 24 August 2005)

We present density matrix renormalization group calculations of the ground-state properties of quarter-filled ladders including static electron-lattice coupling. Isolated ladders and two coupled ladders are considered, with model parameters obtained from band-structure calculations for α' - NaV_2O_5 . The relevant Holstein coupling to the lattice causes static out-of-plane lattice distortions, which appear concurrently with a charge-ordered state and which exhibit the same zigzag pattern observed in experiments. The inclusion of electron-lattice coupling drastically reduces the critical nearest-neighbor Coulomb repulsion V_c needed to obtain the charge-ordered state. No spin gap is present in the ordered phase. The charge ordering is driven by the Coulomb repulsion and the electron-lattice interaction. With electron-lattice interaction, coupling two ladders has virtually no effect on V_c or on the characteristics of the charge-ordered phase. At $V=0.46$ eV, a value consistent with previous estimates, the lattice distortion, charge gap, charge-order parameter, and the effective spin coupling are in good agreement with experimental data for NaV_2O_5 .

DOI: 10.1103/PhysRevB.72.085131

PACS number(s): 71.38.-k, 71.10.Fd, 63.22.+m

I. INTRODUCTION

Since the observation of a phase transition at $T_{\text{CO}} \approx 34$ K via magnetic susceptibility measurements,¹ the physical properties of the low-dimensional inorganic compound, NaV_2O_5 ,² have been investigated intensively. The lattice distortions,³ the opening of a spin gap⁴ at T_{CO} or slightly below,^{5,6} and the static charge disproportion δ between the V ions are the most remarkable properties of this phase transition, which was at first identified as a spin-Peierls transition like that in CuGeO_3 .⁷ Later studies² found that zigzag charge ordering occurs below the phase transition in NaV_2O_5 , which is made up of quarter-filled ladders. It now appears that the opening of the spin gap may be induced primarily by charge transfer⁸⁻¹¹ in the low-temperature superlattice.¹²⁻¹⁶ The discussion on the main driving force of the transition is still going on. It was argued recently that the Coulomb repulsion on an isolated ladder might be too small to cause charge ordering.^{11,17} The interladder coupling, which appears to cause the spin gap, would then also have to be responsible for the charge ordering. However, the electron-lattice coupling has been found to contribute to the charge-ordering transition.¹⁸⁻²³

In this work, we concentrate on the effects of electron-lattice interactions on the ground state of NaV_2O_5 . Due to the asymmetric crystal environment of the V ions in NaV_2O_5 , the strongest lattice coupling is a Holstein-like electron-phonon interaction involving the d_{xy} electrons.^{20,24} We investigate the extended Hubbard model with Holstein coupling, introduced in Ref. 23, using high precision density matrix renormalization group (DMRG) calculations on isolated and on two coupled ladders. We show that, indeed, including the electron-lattice coupling causes charge ordering to appear on isolated as well as on two coupled ladders at significantly smaller Coulomb repulsions, with values which are consistent with most independent estimates.

In Sec. II, we present the model and discuss the parameter values and observables. We discuss results for an isolated

ladder in Sec. III as a function of the nearest-neighbor Coulomb repulsion. Section IV treats coupled ladders and is followed by our conclusions.

II. MODEL

NaV_2O_5 is the only known quarter-filled ladder compound.²⁵ Ladderlike structures are formed by the vanadium ions and are only weakly coupled. A useful microscopic description is provided by an extended Hubbard model (EHM) with Coulomb repulsion between nearest-neighbor sites. The properties of the EHM without electron-lattice coupling were studied using mean field approaches,^{9,26-28} perturbation theory,²⁹ the cluster dynamical mean-field theory,³⁰ exact diagonalization,^{23,28,31-33} bosonization,³⁴ quantum Monte Carlo,³⁵ and cluster perturbation theory.³⁶ Detailed studies of the EHM were also performed using the DMRG,^{37,38} but not at specific values of the coupling parameters appropriate for NaV_2O_5 .

A complete microscopic description of NaV_2O_5 must incorporate the lattice distortion observed by x-ray diffraction in the low-temperature phase.³ The distortions of the vanadium ions considerably change the distance to the neighboring oxygen atoms directly above or below the vanadium site.³ Recent calculations using density functional theory in the local density approximation (LDA) have shown that the main effect of these distortions is a change of the local potentials, i.e., a Holstein-like coupling H_{e-l} .²⁴ Indeed, the corresponding phonons are the strongest-coupling A_g modes²⁴ in NaV_2O_5 ; in the current study, we restrict the electron-lattice coupling to these distortions. The contribution of the lattice deformation to the Hamiltonian can be approximated by a parabolic potential H_l . This yields the microscopic Hamiltonian proposed and studied on small systems in Ref. 23,

$$H = H_{\text{EHM}} + H_l + H_{e-l} \quad (1)$$

with

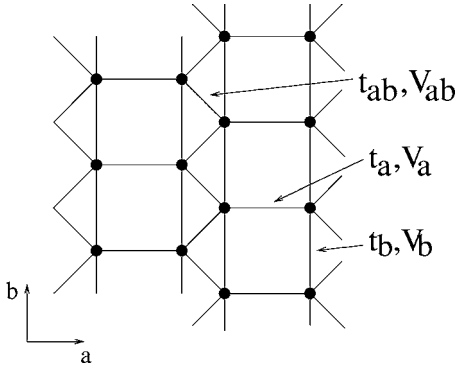


FIG. 1. Schematic depiction of the vanadium ladders in NaV_2O_5 . The three types of hopping matrix elements (t_a, t_b, t_{ab}) and nearest-neighbor Coulomb repulsion (V_a, V_b, V_{ab}) are indicated. Two ladders are shown.

$$H_{\text{EHM}} = - \sum_{(ij), \sigma} t_{ij} (c_{i\sigma}^\dagger c_{j\sigma} + \text{H.c.}) + U \sum_i n_{i\uparrow} n_{i\downarrow} + \sum_{(ij)} V_{ij} n_i n_j, \quad (2a)$$

$$H_l = \kappa \sum_i \frac{z_i^2}{2}, \quad (2b)$$

$$H_{e-l} = -C \sum_i z_i n_i, \quad (2c)$$

where $n_i = n_{i\downarrow} + n_{i\uparrow}$ is the occupation number and z_i the distortion at site i (in units of 0.05 \AA). The Hamiltonian contains the effective lattice force constant κ and a large Holstein constant C . The placement of the hopping terms t_{ij} and the Coulomb repulsion V_{ij} in the lattice structure are depicted in Fig. 1. The parameters are taken from LDA calculations;²⁴ the hopping amplitudes t_{ij} are compatible with earlier calculations.^{25,39} The lattice parameters C and κ were extracted by comparing the total energy and the inter-ionic forces in distorted and undistorted lattices. They correspond to the V—O stretching perpendicular to the ladder plane observed in the 970 cm^{-1} phonon mode. As in Ref. 23, we take

$$t_a = 0.35 \text{ eV} = 2t_b, \quad t_{ab} = 0.17t_a \text{ and } 0.33t_a,$$

$$V_a = V_b = V_{ab} = V, \quad U = 8.0t_a,$$

$$\kappa = 0.125t_a, \quad C = 0.35t_a. \quad (3)$$

We compare results for two different values, $0.17t_a$ and $0.33t_a$, of the interladder hopping because existing estimates of these parameters differ.^{24,25,39} The Coulomb repulsion is very difficult to compute; estimates in the literature vary strongly.^{9,17,28–30,40} In our study, we take $V_a = V_b = V_{ab} = V$ for simplicity, and investigate the model as a function of V .

We have performed DMRG calculations on isolated ladders of length of up to $L=80$ and on two coupled ladders of length of up to $L=24$, applying open boundary conditions

along the chains (b direction). In the case of two coupled ladders, we have taken periodic boundary conditions in the a direction.

We have measured the charge-order parameter m_{CO} , defined by

$$m_{\text{CO}}^2 = \frac{1}{N^2 \langle n \rangle^2} \sum_{ij} e^{i\mathbf{Q}(\mathbf{R}_i - \mathbf{R}_j)} (\langle n_i n_j \rangle - \langle n \rangle^2), \quad (4)$$

where $\mathbf{Q} = (\pi, \pi)$ and N is the total number of sites in the system. The occupation number of the two inequivalent V ions is then $(1 \pm m_{\text{CO}})/2$.

The charge gap $\Delta_C(L)$ and the spin gap $\Delta_S(L)$ are determined using

$$\Delta_C(L) = \frac{1}{2} [E_0(L, N+2) + E_0(L, N-2) - 2E_0(L, N)],$$

$$\Delta_S(L) = E_0(L, N, S_z = 1) - E_0(L, N, S_z = 0), \quad (5)$$

where $E_0(L, N)$ is the ground-state energy of the system with L rungs per ladder and N electrons.³⁸ Results are extrapolated to $L=\infty$ using linear and quadratic fits in $1/L$ and by applying finite-size scaling.

III. ISOLATED LADDER

In this section, we present DMRG calculations on isolated quarter-filled ladders ($V_{ab}=0, t_{ab}=0$). We consider systems with ($C=0.35$) and without ($C=0$) electron-lattice interactions and compare the results.

Isolated quarter-filled ladders without coupling to the lattice were investigated by Vojta *et al.*^{37,38} for a range of parameters. The parameters studied did not, however, include the couplings relevant for NaV_2O_5 , which is characterized by large hopping along the rungs, $t_a \approx 2t_b$, large Coulomb repulsion $U \approx 8t_a$, and charge ordering. Reference 38 found qualitatively different behavior for $t_a \leq t_b$, where the spin gap was found to be finite, and $t_a \geq t_b$, where the spin gap was found to vanish.

In Fig. 2, we display the square of the charge-order parameter m_{CO}^2 as a function of the nearest-neighbor Coulomb repulsion V for different system sizes. At a critical value V_c above $2t_a$, there is a quantum phase transition to a phase with a finite charge order. The essential features of this transition can be described by a model with a single charge degree of freedom on each rung, i.e., a pseudospin. When the hopping between rungs is neglected, one arrives at the Ising model in a transverse field (IMTF),^{9,33} which can be solved exactly.⁴¹ Indeed, a finite-size scaling analysis for m_{CO}^2 in which $L^{2\beta/\nu} m_{\text{CO}}^2$ is plotted as a function of $L^{1/\nu} [(V_c/V) - 1]$ with the critical exponents $\nu=1, \beta=\frac{1}{8}$ of the IMTF, shown in the inset, collapses all data points onto a universal curve and yields a critical Coulomb repulsion of $V_c = 2.31(2)t_a$. We have also performed a similar scaling analysis without fixing ν and β and obtain a reasonable data collapse with $\nu=1.0(1), \beta=0.125(20)$, and $V_c = 2.31(4)$. We note that $\beta=\frac{1}{8}$ (which is also the exponent of the 2D Ising model) is fairly close to the value extracted from experimental results for NaV_2O_5 ,^{5,42}

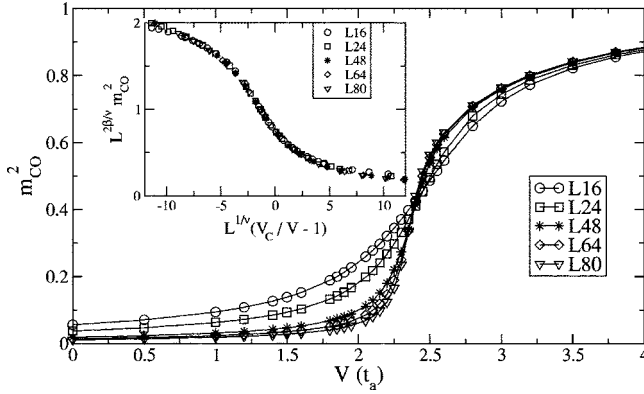


FIG. 2. Square of the charge-order parameter, m_{CO}^2 , on an isolated ladder without coupling to the lattice, as a function of the nearest-neighbor Coulomb repulsion V for several ladder lengths L . The inset shows the finite-size scaling data collapse, with exponents $\nu=1$, $\beta=\frac{1}{8}$, and critical Coulomb repulsion $V_c=2.31(2)$.

about 0.15–0.20. However, the effective Coulomb coupling V in NaV_2O_5 is probably considerably below $V_c \approx 2.31t_a$.^{9,17,28–30,40} Therefore, the Coulomb repulsion alone is insufficient to cause the charge ordering in NaV_2O_5 .

When the electron-lattice coupling is taken into account, the behavior of the charge order parameter changes drastically, as we will now show. The ground-state energy $E_0(\{z_i\})$ of the Hamiltonian H [Eq. (1)] is a function of the independent classical lattice distortions z_i on each site. First, we have determined the optimal distortion pattern on ladders of up to 16 sites using classical Monte Carlo simulations carried out in the space of all z_i .

In these simulations, the ground-state energies are determined by exact diagonalization. We use parallel tempering⁴³ to find all relevant distortion patterns. We find that at low V the optimum lattice distortion (lowest total energy) is $z_i=0$, i.e., no distortion. Above a critical value $V_c \approx 0.95t_a$, there are two degenerate optimal configurations, with finite zigzag lattice distortions

$$z_i = z e^{i\mathbf{Q}\cdot\mathbf{R}_i}, \quad \mathbf{Q} = (\pi, \pi), \quad (6)$$

where \mathbf{R}_i labels the lattice sites. The zigzag pattern of the lattice distortions agrees with the experimentally observed pattern.³ In the following, we therefore assume a zigzag pattern. We determine the ground state by minimizing $E_0(z)$ as a function of the lattice distortion z , similarly to Ref. 23. The position of the minimum defines the optimal distortion z_{opt} .

The optimal distortion z_{opt} and the extrapolation to the thermodynamic limit are presented in Fig. 3. The distortion becomes finite at a critical Coulomb repulsion $V_c=0.95(1)$. From Fig. 3 and from the experimentally determined size of the zigzag distortion,³ ($z_{\text{exp}} \approx 0.85 \times 0.5 \text{ \AA}$), we obtain an estimate for the effective Coulomb repulsion in NaV_2O_5 of $V^* = 1.3t_a$, well within the range of most earlier estimates.^{17,28–30,40}

The square of the charge-order parameter $m_{\text{CO}}^2(L)$, calculated at the optimal distortions $z_{\text{opt}}(L)$, is shown in Fig. 4, along with a finite-size extrapolation. Order sets in at the same V as the lattice distortion z_{opt} . For the $1/L$ -extrapolated

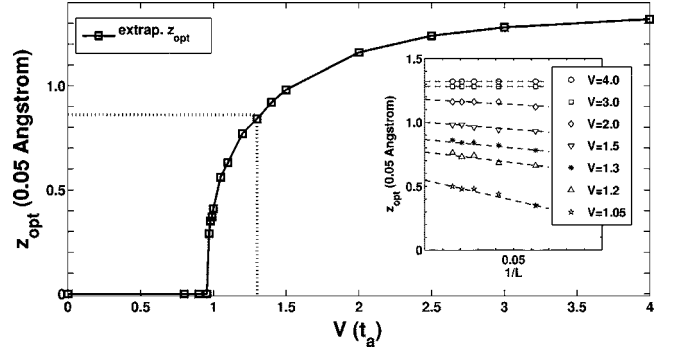


FIG. 3. Optimal zigzag distortion z_{opt} , extrapolated to $L=\infty$, as a function of V on an isolated ladder system with electron-lattice coupling. The inset shows the linear $1/L$ extrapolation for some values of V . The experimentally determined distortion in NaV_2O_5 corresponds to $V^* = 1.3t_a$, indicated by the dotted lines.

values, m_{CO}^2 is proportional to the square of the optimal distortion z_{opt}^2 at all V . In a finite-size scaling analysis (not shown), the scaling of m_{CO} is consistent with the mean-field exponent $\beta=\frac{1}{2}$, but not with the IMTF exponent $\beta=\frac{1}{8}$.

A comparison of Fig. 2 and 4 illustrates the substantial decrease of the critical Coulomb repulsion due to the electron-lattice coupling. The critical value V_c decreases from $V_c=2.31(2)t_a$ without electron-lattice coupling to $V_c=0.95(1)t_a$ with electron-lattice coupling. The critical exponent of m_{CO} is clearly smaller than unity in both cases, but changes from $\beta \approx \frac{1}{8}$ to $\beta \approx \frac{1}{2}$ when the electron-lattice coupling is switched on. At the coupling V^* at which the lattice distortion matches the experiment value, we find $m_{\text{CO}}^2 \approx 0.37$, very close to the experimental results of about 0.35,¹⁰ and 0.37.¹⁴

The charge gap Δ_C is also influenced by the presence of electron-lattice coupling, as shown in Fig. 5. The charge gap increases with increasing V and lattice distortion and does not vanish³⁸ at $V=0$. At $V^* = 1.3t_a$, the charge gap agrees reasonably well with the experimental value for the optical gap in NaV_2O_5 .⁴⁴

The spin gap of an isolated quarter-filled ladder without electron-lattice coupling has been shown by Vojta *et al.*³⁸ to

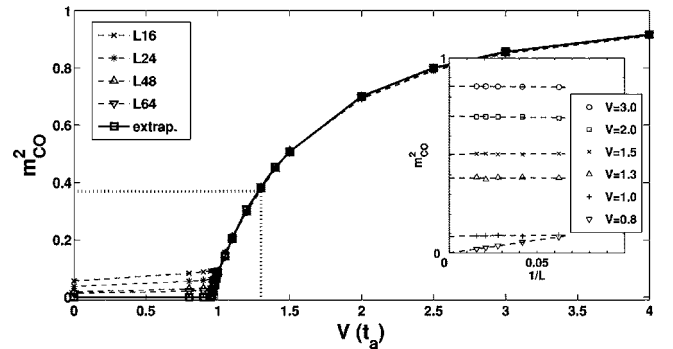


FIG. 4. Square of the charge-order parameter m_{CO}^2 calculated at the optimal distortion z_{opt} on an isolated ladder with electron-lattice coupling as a function of V and for several ladder lengths L . The solid line is the result of a linear $1/L$ extrapolation, illustrated in the inset for selected values of V . The dotted lines mark $V^* = 1.3t_a$.

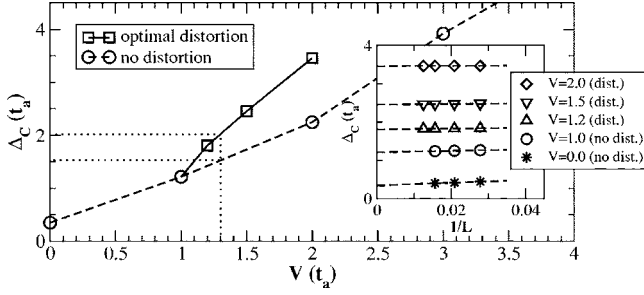


FIG. 5. Charge gap Δ_C on an isolated ladder as a function of V , with (solid) and without (dashed) electron-lattice coupling. The results at $V^* = 1.3t_a$ are indicated by dotted lines. Inset: linear finite-size extrapolation in $1/L$ for systems with (dist.) and without (no dist.) lattice distortion.

vanish at moderate V when the rung hopping t_a is larger than t_b , as is the case in NaV_2O_5 . In Fig. 6(a), we show some representative results of our calculations of the spin gap, with and without electron-lattice coupling, together with a quadratic $1/L$ extrapolation. We find that the *spin gap extrapolates to zero on an isolated ladder at all V in both cases*. Charge ordering on an isolated ladder is therefore not sufficient to induce a spin gap.

The magnetic behavior of the quarter-filled Hubbard ladder can be approximated by an antiferromagnetic Heisenberg model.^{25,38,39} We determine an effective magnetic exchange interaction J_{eff} by equating the finite-size spin gap in our model to that of a Heisenberg chain with exchange constant J , i.e.,

$$\frac{\Delta_S^{\text{Heisenberg}}(L)}{J} = \frac{\Delta_S^{\text{Hubbard}}(L)}{J_{\text{eff}}(L)}. \quad (7)$$

The results are plotted in Fig. 7 as a function of inverse system size $1/L$. There is only a weak L dependence, and the scaling is linear in $1/L$. Previous work using exact diagonalization²³ showed that the behavior of the dynamical spin correlations $S(k, \omega)$ for the EHM with electron-lattice coupling also closely resemble those of the Heisenberg chain. Remarkably, our results for J_{eff} agree very well with the estimates from the spin dispersion in Ref. 23.

The resulting values of J_{eff} are plotted in Fig. 8 as a func-

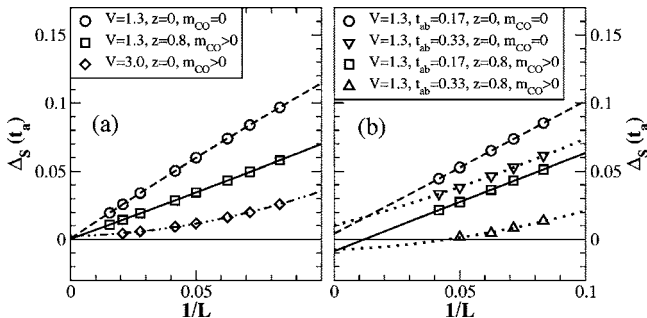


FIG. 6. Spin gap Δ_S for (a) an isolated ladder and (b) two coupled ladders. Lines represent a quadratic fit in $1/L$. The boxed descriptions of the curves are in the same vertical order as the data.

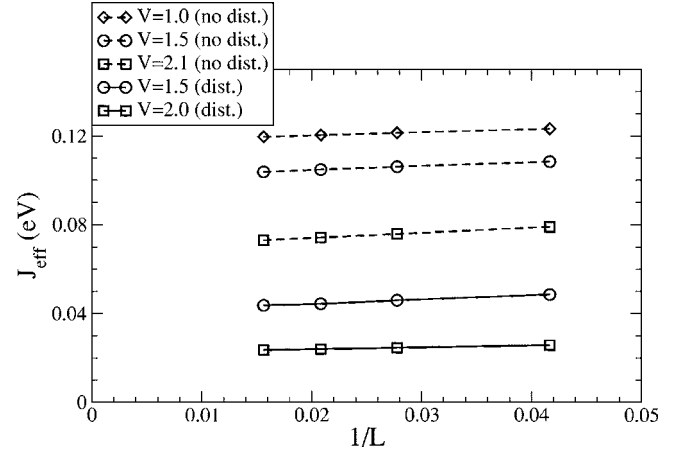


FIG. 7. Effective magnetic exchange coupling J_{eff} [Eq. (7)] as a function of inverse lattice size $1/L$, for different values of V , with and without lattice distortion.

tion of V . As V is increased, the charge-order parameter increases and J_{eff} decreases. This behavior is in accordance with the experimental observation that J_{eff} becomes smaller at lower temperature, where charge order increases. Part of the reduction in J_{eff} is due directly to the charge occupation of neighboring sites along the chains, which implies a reduction by a factor of $(1 - m_{\text{CO}}^2)$.⁸ Our results, however, are far from such a simple quadratic dependence on m_{CO}^2 .

IV. COUPLED LADDERS

The occurrence of a spin gap in NaV_2O_5 may largely be due to the coupling of ladders.⁸⁻¹¹ We have therefore studied a system of two coupled ladders with periodic boundary condition in the a direction. We have determined the pattern of optimal lattice distortions in the same way as for the isolated ladder (for $t_{ab} = 0.33t_a$), using exact diagonalization on a 16-site system, and find a simultaneous zigzag distortion on both ladders to be optimal. Due to the lattice structure (see Fig. 1), the energy is invariant under a shift of the distortion by one rung on either ladder. Using the DMRG, we have then examined larger systems. We have determined the opti-

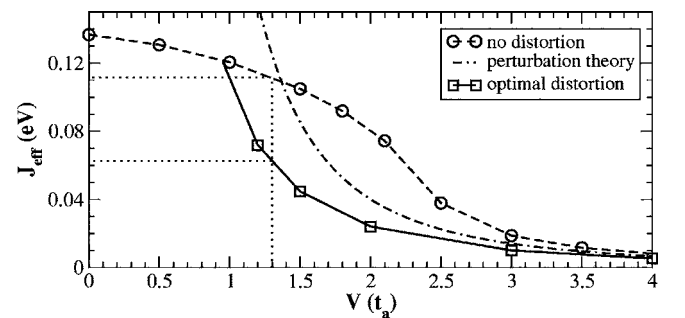


FIG. 8. Effective magnetic exchange coupling J_{eff} on an isolated ladder as a function of V , with (solid line) and without (dashed line) electron-lattice coupling. The dashed-dotted line is the result of perturbation theory (Ref. 38) for the undistorted lattice, valid only at large charge order.

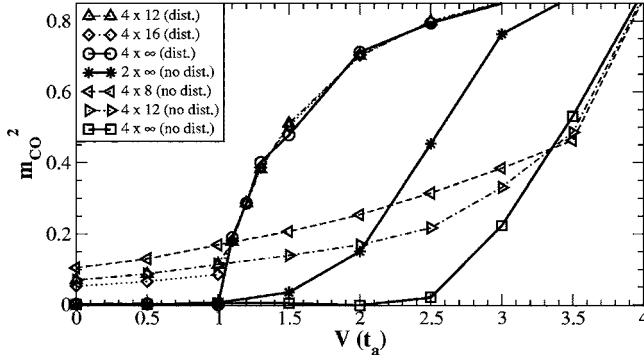


FIG. 9. Square of the charge-order parameter, m_{CO}^2 , for two coupled ladders ($4 \times L, t_{ab} = 0.33t_a$) with periodic boundary conditions in the a direction and with and without lattice distortions. The results for infinite length are obtained using a linear extrapolation in $1/L$. Also included for comparison are similarly extrapolated results for an isolated ladder ($2 \times \infty$).

mal distortion z_{opt} from the minimum of the ground-state energy $E_0(z)$ as a function of the uniform zigzag distortion. The result is very similar to the lattice distortion in the isolated ladder at the same V . The effective Coulomb repulsion determined from the experimental lattice distortion is therefore still $V^* = 1.3t_a$.

Without electron-lattice coupling, convergence of the DMRG calculations is difficult to achieve, restricting the largest length to at most $L=12$ at large V . The three rightmost curves in Fig. 9 show the results for the charge-order parameter as a function of V for lattice sizes $L=8, L=12$, and for a $1/L$ extrapolation. For comparison, the results for a single ladder without electron-lattice coupling extrapolated in the same way are also shown (middle solid line marked with stars). Clearly, the system consisting of two coupled ladders tends to order at even larger values of V than the isolated ladder, leading to an even larger discrepancy with the estimates for V in NaV_2O_5 .

At the lattice sizes we were able to reach, the effects of the open boundaries, especially effects caused by the different number of neighbors at the boundary, are considerable. While varying the boundaries, e.g., compensating for missing neighbors, did affect the results shown in Fig. 9, it did not change the overall tendency to shift the phase transition to larger V .

For systems with electron-lattice coupling, we were able to reach larger sizes, up to 4×16 sites at large V and up to 4×24 at $V^* = 1.3t_a$. The results, as can be seen in Fig. 9, are almost identical to the results on a single ladder of the same length L and are almost independent of length in the ordered phase. Charge ordering still takes place at $V \approx 0.95t_a$.

The spin gap of the coupled ladder system is displayed in Fig. 6(b) for $V^* = 1.3t_a$. Since estimates of the interladder hopping t_{ab} in NaV_2O_5 vary,^{24,25,39} we have performed our calculations for two values, $t_{ab} = 0.17t_a$ and $0.33t_a$. At $t_{ab} = 0.17t_a$, the spin gap for two coupled ladders both with and without lattice distortion is similar in value and finite-size behavior to that for the isolated ladder, which vanishes in the thermodynamic limit. When the interladder hopping is increased to $t_{ab} = 0.33t_a$, the spin gap becomes smaller and its

finite-size dependence appears to change in both cases. The physics of the individual ladders thus appears to be noticeably affected by interladder coupling at this larger hopping.

Extrapolations of the gaps using a fit to a quadratic polynomial in $1/L$ are indicated by the lines in the figure. The value of the spin gap in the $L \rightarrow \infty$ limit for all parameter values is approximately zero, $|\Delta_S(L=\infty)| < 0.01t_a$. Some of the extrapolations in Fig. 6 yield values that are slightly negative. The magnitude of these negative values gives a minimal error estimate for the extrapolation. Since the magnitudes of the positive extrapolations are of similar size, we conclude that the extrapolated spin gaps are zero to within errors. In addition, the small extrapolated gaps are significantly smaller than the spin gap found experimentally in NaV_2O_5 , $\Delta_S \approx 10 \text{ meV} \approx 0.03t_a$. The spin gaps at other values of V ($V = 0.9t_a, 1.5t_a$) behave similarly.

We conclude that when two ladders are coupled, there is no significant indication that a spin gap opens. This result is not unexpected, however, because the mechanism which has been proposed as the cause for the spin gap in the charge-ordered system,⁸⁻¹¹ namely an in-ladder dimerization of effective spin couplings, requires a charge-ordering pattern with a period of *four* ladders in the a direction; such a pattern is observed in NaV_2O_5 .¹²⁻¹⁵

V. CONCLUSIONS

In this paper, we have investigated the influence of Coulomb repulsion and electron-lattice interactions in quarter-filled ladder materials such as NaV_2O_5 by treating the extended Hubbard model with and without coupling to static lattice distortions in the c direction. Our calculations show that the electron-lattice coupling drastically affects the physical properties of the low-temperature phase. It causes lattice distortions to appear concurrently with charge ordering and with the same spatial zigzag pattern. The transition to the charge-ordered phase is shifted to a much smaller critical value of the nearest-neighbor Coulomb repulsion ($V_c \approx 0.95t_a$). The charge gap is increased and the effective magnetic exchange is reduced by the electron-lattice coupling. These results remain unchanged when two ladders are coupled. The spin gap extrapolates to zero in all cases.

When the electron-lattice coupling is included, the properties of both the isolated ladder and two coupled ladders are in remarkably good agreement with experimental data for NaV_2O_5 , at an effective Coulomb repulsion $V^* = 1.3t_a$ deter-

TABLE I. Comparison of experimental data for NaV_2O_5 to the results for the extended Hubbard model with lattice coupling, at $V^* = 1.3t_a$.

	EHM+Lattice $V=1.3t_a$	Experimental Data
Distortion/0.05 Å	0.84	0.85, Ref. 3
m_{CO}^2	0.37	0.35–0.37, Refs. 10 and 14
J_{eff}	63 meV	60 meV, Ref. 10
Δ_c	0.7 eV	0.9 eV, Ref. 44

mined by matching the experimental lattice distortion. This Coulomb repulsion is well within the range previously estimated for NaV_2O_5 . As shown in Table I, we find simultaneous agreement for the zigzag distortion, the size of the charge-order parameter, the effective spin interaction, and the charge gap with experimental data.

While results for the isolated ladder without electron-lattice coupling would also be reasonably consistent with the experimental values, an unrealistically large value for the Coulomb repulsion, $V \approx 2.5t_a$, would be required, and the experimentally observed lattice distortion would not be present. The value of the Coulomb repulsion necessary for such an agreement becomes still larger when two ladders without electron-lattice interaction are coupled.

We conclude that an interplay of charge ordering and lattice distortion can drive the phase transition to a charge-ordered state in NaV_2O_5 , independent of the occurrence of a spin gap. The explanation of the spin gap will likely require a unit cell with at least four coupled ladders. Corresponding work is in progress.

ACKNOWLEDGMENTS

This work has been supported by the Austrian Science Fund FWF, Project No. P15520. The authors would like to thank M. Aichhorn, C. Gros, T. C. Lang, F. Michel, and E. Sherman for stimulating discussions.

-
- ¹M. Isobe and Y. Ueda, *J. Phys. Soc. Jpn.* **65**, 1178 (1996).
²For a review, see P. Lemmens, G. Güntherodt, and C. Gros, *Phys. Rep.* **375**, 1 (2003).
³J. Lüdecke, A. Jobst, S. van Smaalen, E. Morré, C. Geibel, and H.-G. Krane, *Phys. Rev. Lett.* **82**, 3633 (1999).
⁴T. Yoshihama, M. Nishi, K. Nakajima, K. Kakurai, Y. Fujii, M. Isobe, C. Kagami, and Y. Ueda, *J. Phys. Soc. Jpn.* **67**, 744 (1998).
⁵Y. Fagot-Revurat, M. Mehring, and R. K. Kremer, *Phys. Rev. Lett.* **84**, 4176 (2000).
⁶M. Köppen, D. Pankert, R. Hauptmann, M. Lang, M. Weiden, C. Geibel, and F. Steglich, *Phys. Rev. B* **57**, 8466 (1998).
⁷M. Hase, I. Terasaki, and K. Uchinokura, *Phys. Rev. Lett.* **70**, 3651 (1993).
⁸C. Gros and R. Valentí, *Phys. Rev. Lett.* **82**, 976 (1999).
⁹M. Mostovoy and D. I. Khomskii, *Solid State Commun.* **113**, 159 (2000); M. V. Mostovoy, D. I. Khomskii, and J. Knoester, *Phys. Rev. B* **65**, 064412 (2002).
¹⁰B. Grenier, O. Cepas, L. P. Regnault, J. E. Lorenzo, T. Ziman, J. P. Boucher, A. Hiess, T. Chatterji, J. Jegoudez, and A. Revcolevschi, *Phys. Rev. Lett.* **86**, 5966 (2001).
¹¹C. Gros and G. Y. Chitov, *Europhys. Lett.* **69**, 447 (2005).
¹²S. van Smaalen, P. Daniels, L. Palatinus, and R. K. Kremer, *Phys. Rev. B* **65**, 060101(R) (2002).
¹³S. Grenier, A. Toader, J. E. Lorenzo, Y. Joly, B. Grenier, S. Ravy, L. P. Regnault, H. Renevier, J. Y. Henry, J. Jegoudez, and A. Revcolevschi, *Phys. Rev. B* **65**, 180101(R) (2002).
¹⁴H. Sawa, E. Ninomiya, T. Ohama, H. Nakao, K. Ohwada, Y. Murakami, Y. Fujii, Y. Noda, M. Isobe, and Y. Ueda, *J. Phys. Soc. Jpn.* **71**, 385 (2002).
¹⁵K. Ohwada, Y. Fujii, Y. Katsuki, J. Muraoka, H. Nakao, Y. Murakami, H. Sawa, E. Ninomiya, M. Isobe, and Y. Ueda, *Phys. Rev. Lett.* **94**, 106401 (2005).
¹⁶G. Y. Chitov and C. Gros, *J. Phys.: Condens. Matter* **16**, L415 (2004).
¹⁷D. Sa and C. Gros, *Eur. Phys. J. B* **18**, 421 (2000).
¹⁸M. Fischer, P. Lemmens, G. Els, G. Güntherodt, E. Ya. Sherman, E. Morré, C. Geibel, and F. Steglich, *Phys. Rev. B* **60**, 7284 (1999).
¹⁹J. Riera and D. Poilblanc, *Phys. Rev. B* **59**, 2667 (1999).
²⁰E. Ya. Sherman, M. Fischer, P. Lemmens, P. H. M. van Loosdrecht, and G. Güntherodt, *Europhys. Lett.* **48**, 648 (1999).
²¹A. Bernert, P. Thalmeier, and P. Fulde, *Phys. Rev. B* **66**, 165108 (2002).
²²R. T. Clay and S. Mazumdar, cond-mat/0305479 (unpublished).
²³M. Aichhorn, M. Hohenadler, E. Ya. Sherman, J. Spitaler, C. Ambrosch-Draxl, and H. G. Evertz, *Phys. Rev. B* **69**, 245108 (2004).
²⁴J. Spitaler, E. Ya. Sherman, C. Ambrosch-Draxl, and H. G. Evertz, *Phys. Scr.*, T **T109**, 159 (2004); J. Spitaler, E. Ya. Sherman, H. G. Evertz, and C. Ambrosch-Draxl, *Phys. Rev. B* **70**, 125107 (2004).
²⁵H. Smolinski, C. Gros, W. Weber, U. Peuchert, G. Roth, M. Weiden, and C. Geibel, *Phys. Rev. Lett.* **80**, 5164 (1998).
²⁶H. Seo and H. Fukuyama, *J. Phys. Soc. Jpn.* **67**, 2602 (1998); *J. Phys. Chem. Solids* **60**, 1095 (1999).
²⁷P. Thalmeier and P. Fulde, *Europhys. Lett.* **44**, 242 (1998).
²⁸M. Cuoco, P. Horsch, and F. Mack, *Phys. Rev. B* **60**, R8438 (1999).
²⁹V. Yushankhai and P. Thalmeier, *Phys. Rev. B* **63**, 064402 (2001).
³⁰V. V. Mazurenko, A. I. Lichtenstein, M. I. Katsnelson, I. Dasgupta, T. Saha-Dasgupta, and V. I. Anisimov, *Phys. Rev. B* **66**, 081104(R) (2002).
³¹A. Hübsch, C. Waidacher, K. W. Becker, and W. von der Linden, *Phys. Rev. B* **64**, 075107 (2001); *Physica B* **312**, 626 (2002).
³²A. Hübsch, C. Waidacher, and K. W. Becker, *Phys. Rev. B* **64**, 241103(R) (2001).
³³M. Aichhorn, P. Horsch, W. von der Linden, and M. Cuoco, *Phys. Rev. B* **65**, 201101(R) (2002).
³⁴E. Orignac and R. Citro, *Eur. Phys. J. B* **33**, 419 (2003).
³⁵C. Gabriel, E. Sherman, T. C. Lang, M. Aichhorn, and H. G. Evertz, *Physica B* **359**, 1400 (2005).
³⁶M. Aichhorn, E. Ya. Sherman, and H. G. Evertz, cond-mat/0409162 (unpublished).
³⁷M. Vojta, R. E. Hetzel, and R. M. Noack, *Phys. Rev. B* **60**, R8417 (1999).
³⁸M. Vojta, A. Hübsch, and R. M. Noack, *Phys. Rev. B* **63**, 045105 (2001).
³⁹P. Horsch and F. Mack, *Eur. Phys. J. B* **5**, 367 (1998).
⁴⁰A. N. Yaresko, V. N. Antonov, H. Eschrig, P. Thalmeier, and P. Fulde, *Phys. Rev. B* **62**, 15538 (2000).

- ⁴¹E. Lieb, T. Schultz, and D. Mattis, *Ann. Phys.* **16**, 407 (1961); T. H. Niemeijer, *Physica (Amsterdam)* **36**, 377 (1967); P. Pfeuty, *Ann. Phys.* **57**, 79 (1970).
- ⁴²S. Ravy, J. Jegoudez, and A. Revcolevschi, *Phys. Rev. B* **59**, R681 (1999); B. D. Gaulin, M. D. Lumsden, R. K. Kremer, M. A. Lumsden, and H. Dabkowska, *Phys. Rev. Lett.* **84**, 3446 (2000).
- ⁴³E. Marinari, cond-mat/9612010 (unpublished); Y. Iba, *Int. J. Mod. Phys. C* **12**, 623–656 (2001).
- ⁴⁴C. Presura, D. van der Marel, A. Damascelli, and R. K. Kremer, *Phys. Rev. B* **61**, 15762 (2000).